

The Lorenz number in CeCoIn₅ inferred from the thermal and charge Hall currents

Y. Onose¹, N. P. Ong¹ and C. Petrovic²

¹*Department of Physics, Princeton University, Princeton, NJ 08544, USA*

²*Department of Physics, Brookhaven National Laboratory, Upton, N.Y. 11973, USA*

(Dated: September 2, 2021)

The thermal Hall conductivity κ_{xy} and Hall conductivity σ_{xy} in CeCoIn₅ are used to determine the Lorenz number \mathcal{L}_H at low temperature T . This enables the separation of the observed thermal conductivity into its electronic and non-electronic parts. We uncover evidence for a charge-neutral, field-dependent thermal conductivity, which we identify with spin excitations. At low T , these excitations dominate the scattering of charge carriers. We show that suppression of the spin excitations in high fields leads to a steep enhancement of the electron mean-free-path, which leads to an interesting scaling relation between the magnetoresistance, thermal conductivity and σ_{xy} .

PACS numbers: 71.27.+a,72.15.Eb,72.20.My,74.70.Tx

I. INTRODUCTION

The heavy-electron system CeCoIn₅ exhibits a host of unusual electronic properties of current interest. In the superconducting state, strong evidence for d -wave pairing symmetry has been reported [1, 2, 3, 4, 5]. The FFLO state involving pairing with unequal spin populations in an in-plane magnetic field ($\mathbf{H} \perp \mathbf{c}$) has been proposed [6]. The phase diagram in a perpendicular field ($\mathbf{H} \parallel \mathbf{c}$) has also received wide attention [7, 8]. In an extended region in T - H plane surrounding the superconducting (SC) state (labelled I in Fig. 1a), the resistivity ρ and heat capacity exhibit distinctive “non-Fermi liquid” characteristics: $\rho \sim T$ [7], while the Sommerfeld parameter $\gamma(T) \sim \log T$ [8]. When H exceeds the boundary $H_s(T)$, ρ recovers the Fermi-liquid form $\rho = \rho_0 + AT^2$ and the unconventional features of $\gamma(T)$ are suppressed. The high-field region (labelled II in Fig. 1a) is called the Fermi-liquid region. The boundary field $H_s(T)$ and the upper critical field H_{c2} terminate at a quantum critical point (QCP) as $T \rightarrow 0$ (the field scale H_Z is discussed below). Several parameters characterizing resistivity display divergent behavior as the QCP is approached [7]. In addition, a large Nernst signal is observed in I [9, 10].

To clarify the electronic state in the region I, we have measured extensively the in-plane thermal conductivity $\kappa \equiv \kappa_{xx}$ with $\mathbf{H} \parallel \mathbf{c} \parallel \mathbf{z}$, and the thermal Hall conductivity κ_{xy} (the Righi-Leduc effect) in crystals with very long electron mean-free-path ℓ . In addition, we measured the electrical conductivity $\sigma \equiv \sigma_{xx}$ and Hall conductivity σ_{xy} . The crystals, grown from metallic flux [1], are plate-like with the c axis normal to the broadest faces and the a axis along one edge (for structure, see Ref. [11]). The zero-field κ displays a prominent peak below T_c (solid circles in Fig. 1b), which arises from the steep increase in ℓ of Bogolyubov excitations in the superconducting state. Using the Hall conductivities κ_{xy} and σ_{xy} , we demonstrate the validity of the Wiedemann-Franz (WF) law, and then use the Lorenz number to separate the total κ into its electronic and non-electronic components κ_e and κ_b , respectively. From the strong field dependence observed in κ_b , we infer that spin excitations provide the

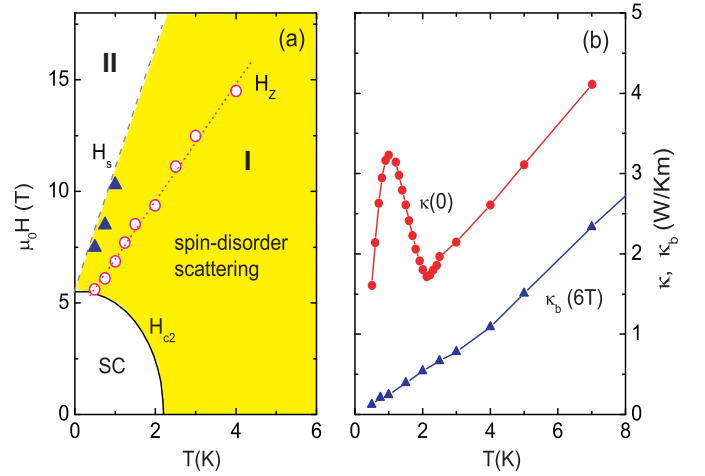


FIG. 1: (a) The phase diagram of CeCoIn₅ adapted from Refs. [7, 8], showing some features inferred from our experiment. The dashed line is the boundary $H_s(T)$ between the Fermi liquid (II) and non-Fermi Liquid (I) regions reported in Refs [7, 8]. Solid triangles are our values for $H_s(T)$. Open circles indicate the field scale H_Z (this work) above which the current ratio $\mathcal{R}_\sigma = Z$ (see Eq. 3). (b) The T dependence of κ in zero field (solid circles) showing a large qp peak below T_c . The background term κ_b measured at 6 T is shown as solid triangles. Below ~ 8 K, κ_b is largely comprised of a term κ_s that is very field dependent (and identified with spin excitations).

dominant scattering mechanism for the charge carriers in the region I. The application of an intense field leads to suppression of this scattering channel and a sharp increase in ℓ . This insight sheds light on the large magnetoresistance and the unusual features of the Hall effect. We discuss the implications for Cooper pairing in the SC region.

II. THERMAL AND CHARGE CONDUCTIVITY TENSORS

The thermal resistivity tensor W_{ij} is measured by applying a weak gradient ($\delta T \sim 10$ mK along length of the crystal at 0.5 K). Below 2 K, the strong variation of ℓ with T and H is potentially the largest source of error in comparing W_{ij} (measured in finite δT) with ρ_{ij} ($\delta T = 0$). We minimized the uncertainties by extensive calibration of the RuO_x thermometers (glued to the crystal), and using very slow field scans (0.1-0.2 T/min. at 0.5 K).

We emphasize that, because ℓ attains very large values below 10 K, it is necessary to use the full matrix inversion to reliably convert the measured tensors W_{ij} and ρ_{ij} into their reciprocal conductivity tensors, e.g. $\kappa_{xx} = W_{xx}/(W_{xx}^2 + W_{xy}^2)$. Experimentally, this means that κ and σ in strong fields cannot be obtained without measuring simultaneously the diagonal and off-diagonal elements of W_{ij} and ρ_{ij} (leaving out the Hall tensor elements leads to errors in κ and σ of 30% or more at low T).

Figure 2 compares the field dependences of κ (Panel a) and the in-plane resistivity ρ (Panel b) at temperatures from 5 K to 0.5 K with $\mathbf{H}||\mathbf{c}$. Above 5 K, an increasing field decreases slightly the observed κ . With decreasing T , however, this trend changes. At 2 K, κ rises gradually with H . At even lower T (0.5–1.5 K), this rising trend becomes firmly established in the normal state when H exceeds H_{c2} (step in κ). In the SC region below H_{c2} , a prominent feature in κ is the sharp, narrow spike which represents the rapid field suppression of the zero-field peak caused by scattering of Bogolyubov excitations from vortices [12, 13, 14]. The spike in κ vs. H below T_c is much larger than previously reported [3]. This reflects a much longer ℓ in the present samples.

The complicated behavior of $\kappa(T, H)$ arises because it is the sum of the electronic term κ_e and a “background” term κ_b carried by charge-neutral excitations (spin excitations and phonons), viz.

$$\kappa(T, H) = \kappa_e(T, H) + \kappa_b(T, H). \quad (1)$$

Our main finding is that, in CeCoIn₅, the charge-neutral term $\kappa_b(T, H)$ displays an unexpectedly strong H dependence. Its T -profile at $H = 6$ T is shown as solid triangles in Fig. 1b.

As previously found [7, 15], CeCoIn₅ exhibits a large magnetoresistance (MR) (Fig. 2b). The initial positive MR ($H < 3$ T) is caused by suppression of superconducting fluctuations which we discuss elsewhere [10]. Our focus is on the negative MR that prevails for $H > 4$ T at all T below ~ 30 K. As T decreases towards T_c , the negative MR becomes pronounced. At 2 K, ρ decreases by ~ 2.5 when H reaches 14 T. Both the sign and magnitude preclude classical MR associated with the Lorentz force. As shown below, the MR results from a steep enhancement of ℓ with increasing field.

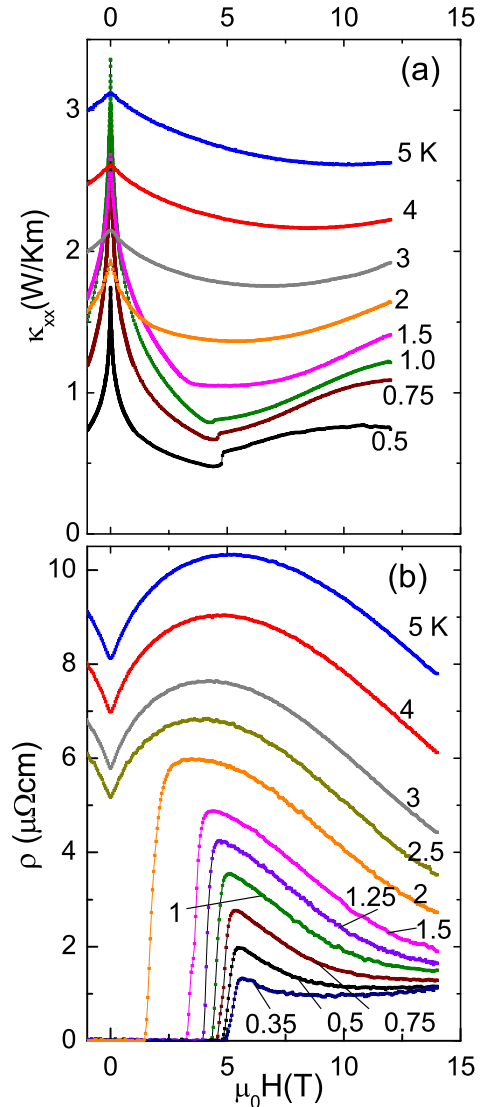


FIG. 2: (a) Curves of κ_{xx} vs. $\mathbf{H}||\mathbf{c}$ at selected T . The steep suppression of the zero-field anomaly produces a sharp spike at each $T < T_c$. (b) The magnetoresistance (MR) ρ vs. $\mathbf{H}||\mathbf{c}$ showing the strong negative MR above 4 or 5 T.

III. LORENZ NUMBER FROM SCALING OF κ_{xy}/T TO σ_{xy}

The field enhancement of ℓ strongly influences the field profiles of the heat and charge currents. To disentangle these effects, we exploit the WF law, which states that the ratio $\kappa_e/T\sigma$ is close to the Lorenz factor $\mathcal{L}_0 = \frac{1}{3}\pi^2(k_B/e)^2$. In the elemental metals, the WF law is nearly universally obeyed at 300 K as well as in the impurity-scattering regime below 4 K, while deviations are common in between. However, in many interesting metals with low carrier densities, κ_e cannot be measured

directly because the charge-neutral term κ_b (usually from phonons) is comparable in size or larger.

Recently, a way to separate κ_e from κ using the Righi-Leduc effect was introduced. Zhang *et al.* [16] have shown that the Lorenz ratio may be determined from the ratio $\mathcal{L}_H \equiv \kappa_{xy}/T\sigma_{xy}$. (Essentially, the Righi-Leduc effect senses only the electronic entropy current, while filtering out the charge-neutral components which do not have a Hall response. Since the latter also do not contribute to σ_{xy} , the ratio of the 2 Hall currents yields the WF ratio. The WF-Hall method was tested on high-purity Cu and applied to cuprates [16].) CeCoIn₅ is well-suited for this method because the 2 Hall conductivities are large.

The Hall resistivity in CeCoIn₅ was previously reported [15], but it is the Hall conductivity that is of interest here. At each T , we find that the profile of σ_{xy} vs. H matches that of κ_{xy} even when the two curves display strong curvature vs. H . The curves of κ_{xy}/T and $\mathcal{L}_H\sigma_{xy}$ are plotted together in Fig. 3 for $T \leq 3$ K (Panel a), and $T > 3$ K (b). Let us first note that the curves share 2 characteristics rarely seen in Hall experiments. In weak H , the curves rise from zero with strong negative curvature to produce a knee-like feature. In addition, the curvature changes its sign to positive in higher fields; both Hall conductivities increase more rapidly than the first power in H in strong fields. Further, we note the peak anomaly in weak H shown by κ_{xy} below 1.5 K. We return to these unusual features later.

At each T , κ_{xy}/T and $\mathcal{L}_H\sigma_{xy}$ may be scaled together over the entire field range by adjusting \mathcal{L}_H . We emphasize that \mathcal{L}_H is an H -independent scaling parameter (otherwise, it does not make sense to discuss scaling between κ_{xy}/T and σ_{xy}). In view of the pronounced nonlinearity, the close match between the 2 field profiles is strong evidence that the WF law is valid with a field-independent Lorenz number. The inferred values of \mathcal{L}_H are plotted in Fig. 4. Between 2 and 10 K, $\mathcal{L}_H/(k_B/e)^2$ is close to the Sommerfeld value $\pi^2/3$, but seems to deviate slightly downwards below 2 K.

IV. SEPARATION OF ELECTRONIC AND NON-ELECTRONIC HEAT CURRENTS

We next determine $\kappa_e(T, H)$ and $\kappa_b(T, H)$ in Eq. 1. Using the values of \mathcal{L}_H in Fig. 4, we convert the measured σ into $\kappa_e(T, H)$ via

$$\kappa_e(T, H) = T\sigma(T, H)\mathcal{L}_H(T). \quad (2)$$

Subtracting the curve of $\kappa_e(T, H)$ from $\kappa(T, H)$ at each T , we finally determine $\kappa_b(T, H)$, which is plotted in Fig. 5a.

At low T , κ_b is found to be strongly H dependent. In general, κ_b is the sum of the spin-excitation conductivity κ_s and the phonon conductivity κ_{ph} , viz. $\kappa_b(T, H) = \kappa_s(T, H) + \kappa_{ph}(T)$. When spin-disorder scattering of phonons is important, an applied field generally leads to an *increase* in κ_{ph} because H suppresses spin disorder,

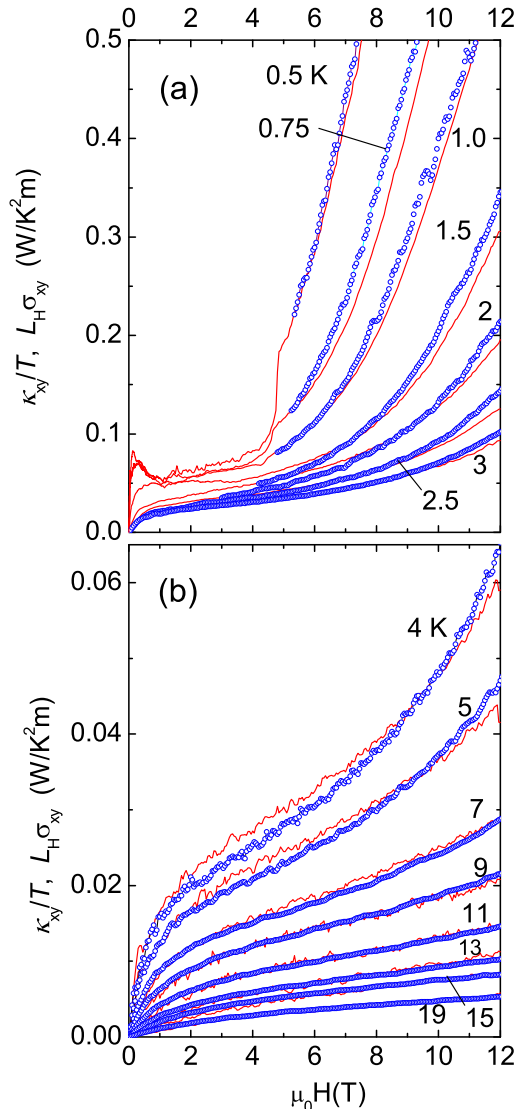


FIG. 3: Comparison of the thermal Hall conductivity κ_{xy}/T (solid curve) and the Hall conductivity σ_{xy} (open circles) scaled by an H -independent \mathcal{L}_H at $T \leq 3$ K (Panel a) and $T > 3$ K (Panel b). Below 1.5 K (Panel a), κ_{xy}/T displays a peak anomaly in weak H . Both Hall currents are electron-like in sign.

which is opposite to what is observed. Consequently, we identify all the field dependence with the spin-excitation term $\kappa_s(T, H)$. Figure 5a shows that κ_s accounts for a large fraction of κ_b between 5 K and 1 K. At the lowest T (0.5–1.5 K), the curve of κ_b falls to a floor value at the field scale $H_s(T)$, which is observable as a break-in-slope. In the phase diagram in Fig. 1a, $H_s(T)$ is seen to lie close to the I/II boundary (solid triangles). With the present data, we cannot determine H_s above 1.5 K. Nonetheless, the trends of the curves in Fig. 1a suggest

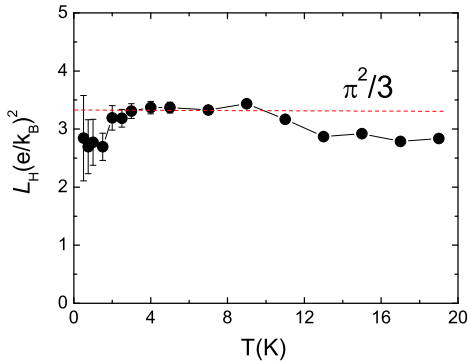


FIG. 4: The Lorenz number \mathcal{L}_H obtained by scaling κ_{xy}/T to σ_{xy} in Fig. 3. \mathcal{L}_H is plotted in units of $(k_B/e)^2$. The dashed line is the Sommerfeld value $\pi^2/3$.

that, throughout the region I up to 5 K, κ_b is greatly reduced from its zero-field values when H reaches the I/II boundary in the phase diagram (Fig. 1a).

We compare our results with Ref. [17], where the Lorenz number was found by estimating the phonon term κ_{ph} from measurements on a La-doped sample [18]. The authors compute κ_e as the difference $\kappa(H, T) - \kappa_{ph}(T)$, assuming κ_{ph} to be strictly H -independent. The inferred Lorenz number \mathcal{L}_{eff} is reported to be suppressed by $\sim 30\%$ in a 10-T field [17], in contrast with our H -independent Lorenz number. The field dependence of \mathcal{L}_{eff} in Ref. [17] comes from identifying κ_b entirely with κ_{ph} which is assumed H -independent. However, we note that the strong H dependence of L_{eff} [17] is mainly observed below our temperature range. Differences at higher T may stem from identifying bosonic contribution through experiments on doped samples [19], as opposed to the Hall response here. In both cases, the Lorenz ratio attains the Sommerfeld value above 4 K.

V. SPIN DEGREES AND CHARGE TRANSPORT

In a conventional magnet, an external \mathbf{H} raises the magnon dispersion energy which reduces the spin-wave population and their thermal conductivity. In the region I of CeCoIn₅, the uniform susceptibility χ is strongly enhanced, but conventional long-range magnetic order seems to be absent. However, in heavy fermions, spin-ordered states involving the local moments in the f bands are widely postulated. Incipient spin ordering may exist above T_c in CeCoIn₅ (see Broholm [20]). Although our analysis is guided by the known properties of conventional spin waves, a more exotic kind of spin ordering is not precluded, and κ_s may derive from spin-excitations in unconventional spin-ordered states. Because of hybridization between the f and s - p - d states and large spin-

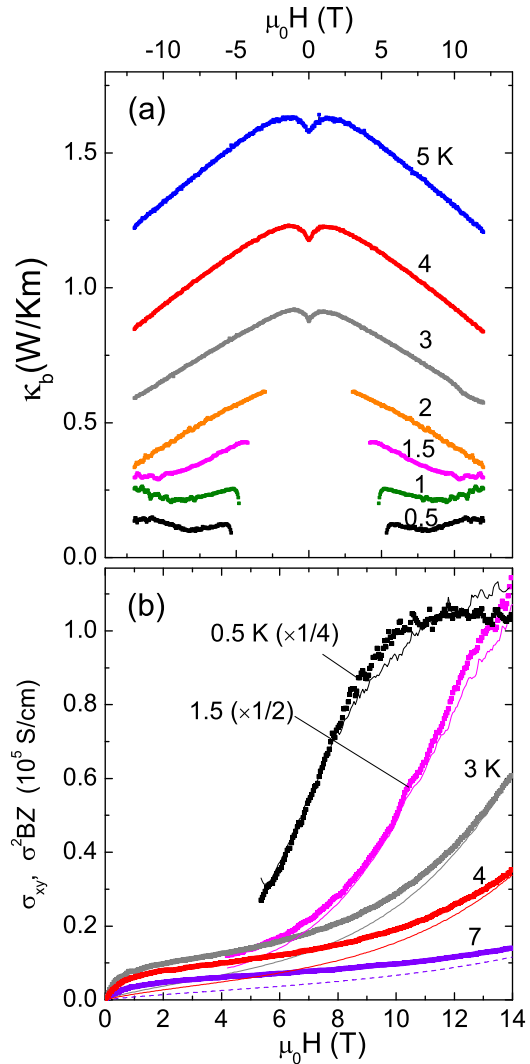


FIG. 5: (a) The curves of $\kappa_b = \kappa_s + \kappa_{ph}$ vs. H obtained by subtracting κ_e from the observed κ at each T (κ_b is not obtained below H_{c2} because $\rho = 0$). At 0.5, 0.75 and 1 K, the H dependence shows a kink at $H = H_s(T)$ at the boundary between I and II (Fig. 1a). The curve of κ_b vs. T at 6 T is shown in Fig. 1b. (b) Comparison of σ_{xy} (bold curves) with the quantity $\sigma^2 B Z$ (thin curves). Above the field $H_Z(T)$, the 2 quantities match over nearly 2 decades with one scaling constant $Z = 1 \times 10^{-7} \text{ cm}^3/\text{C}$. Below H_Z , however, the scaling is spoiled by an “excess Hall current”.

orbit coupling, the spin excitations will strongly scatter the charge carriers. We write $\kappa_s = \frac{1}{3} c_s v \lambda$ where c_s is the heat capacity of the spin excitations, v the average velocity and λ their mean free path. As the local moments align with \mathbf{H} , the spin excitation population $n_s \sim c_s$ decreases steeply in field. We interpret the curves of κ_b in Fig. 5a as the sharp field-suppression of n_s at low T . While evidence for heat currents carried by spin excita-

tions have been reported for low-dimensional oxides [21], a distinguishing feature in CeCoIn_5 is that changes in κ_s strongly affect the charge currents, which we describe next.

The curves in Fig. 5a reveal that the charge-neutral conductivity κ_b decreases strongly with increasing H . This trend is opposite to that in the electronic conductivity σ . As the former decreases, the latter rises in almost direct proportion. [The ratio of $\kappa_b(H)$ evaluated at $H = 0$ and 14 T, $\kappa_b(0)/\kappa_b(14) \sim 1.5$ and 2.7 at 5 K and 2 K, respectively. These ratios match the corresponding ratios $\rho(0)/\rho(14)$ at the same T in Fig. 2b.] Panel b of Fig. 5 shows the steep increase of σ^2 and σ_{xy} with H . As discussed above, the sharp decrease in κ_b with H reflects a decrease in the density of spin excitations n_s . Hence the correlated increase in σ implies that spin excitations are the dominant scattering mechanism of the carriers at these temperatures. The steep increase in ℓ in high field is caused by field-suppression of the spin excitations. Full suppression of this scattering channel, attained when H reaches H_s , leads to the unusually large ℓ in the region II.

VI. MAGNETORESISTANCE AND CURRENT RATIO \mathcal{R}_σ

We have also found that the strong enhancement of ℓ forges a link between the unusual MR and Hall effect. The observed σ_{xy} is the sum of contributions σ_{xy}^i from each FS sheet i . Assuming that the lifetime τ_i on each sheet is dominated by spin-disorder scattering, all τ_i follow the same monotonically rising function of field $g(B)$. As a result, we have $\sigma_{xy} \sim Bg(B)^2$, while the conductivity $\sigma \sim g(B)$: The Hall current grows in direct proportion to the square of the longitudinal current multiplied by B .

To test this assumption, we compare the curves of σ_{xy} with $\sigma^2 B$ at low T (Fig. 5b). In high fields, the quantity $\sigma^2 B \mathcal{Z}$ (thin curves) can be made to match σ_{xy} (bold curves) by setting the T -independent constant $\mathcal{Z} = 1 \times 10^{-7} \text{ cm}^3/\text{C}$. The match is excellent for fields above a cross-over field $H_Z(T)$. As H decreases below H_Z , however, σ_{xy} increasingly exceeds $\sigma^2 B \mathcal{Z}$. The negative curvature (knee) feature described earlier now appears as a small “excess” Hall current below H_Z .

This high-field scaling is made more apparent if we plot the quantity

$$\mathcal{R}_\sigma(T, B) = \sigma_{xy}/\sigma^2 B, \quad (3)$$

which measures the ratio of the Hall current and the longitudinal current squared (see Fig. 6). We note that $\mathcal{R}_\sigma = R_H[1 + (\tan \theta_H)^2]$ deviates from the ordinary Hall coefficient R_H when the Hall angle θ_H is large. Remarkably, Fig. 6 shows that, below 1 K, \mathcal{R}_σ is just a constant equal to \mathcal{Z} , even though both σ and σ_{xy} are increasing with strong curvature. Above 1 K, \mathcal{R}_σ deviates significantly from \mathcal{Z} as the excess Hall current grows, but only for fields $H < H_Z$. Above H_Z (arrow), we see that \mathcal{R}_σ

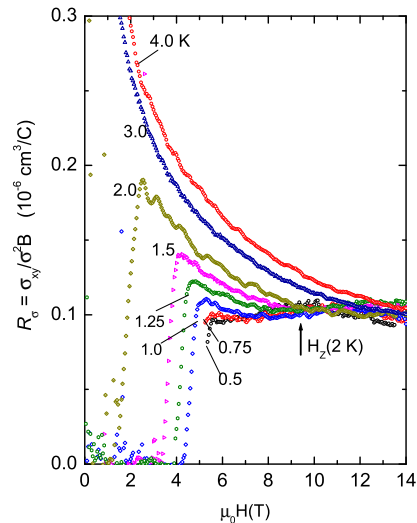


FIG. 6: Curves of the current ratio \mathcal{R}_σ (Eq. 3) at selected T . Above $H_Z(T)$, \mathcal{R}_σ attains a plateau value \mathcal{Z} which is T -independent at our resolution (arrow indicates H_Z at 2 K). The steep variation in weak H reflects the excess Hall current discussed in Fig. 5b.

again settles down to the value \mathcal{Z} . The constancy of \mathcal{R}_σ is direct evidence that both the anomalous MR and σ_{xy} reflect the enhancement in ℓ . As seen in the phase diagram Fig. 1a, H_Z (open circles) lies significantly below H_s . The simple Hall response determines the high-field Hall behavior in the regions I and II. Hence the complicated Hall response in CeCoIn_5 arises solely from the excess Hall current which is responsible for the weak-field “knee”, but is suppressed above H_Z .

VII. QUASIPARTICLES IN SUPERCONDUCTING STATE

These findings have interesting implications for the superconducting state. In heavy-electron systems, pairing mediated by the exchange of spin fluctuations has been proposed as the likely mechanism for the SC state. However, the evidence to date for spin exchange has been indirect. Here, we have exploited the unusually large strong H dependence of the tensors κ_{ij} and σ_{ij} to show that spin excitations in fact provide the dominant scattering channel at low T . Insofar as pairing likely arises from the dominant scattering channel, our results provide rather direct evidence for spin-mediated pairing.

Finally, we comment on the extraordinary peak in κ vs. H that appears below T_c (Fig. 7). The sharp reduction of the peak amplitude in H is very similar to the κ vs. H curves below T_c in untwinned $\text{YBa}_2\text{Cu}_3\text{O}_7$ (YBCO) [13]. The extreme sensitivity to H is interpreted as caused by scattering of nodal qp by vortices [12, 13, 14]. In YBCO, the observation of a large anomaly in κ_{xy} that peaks at

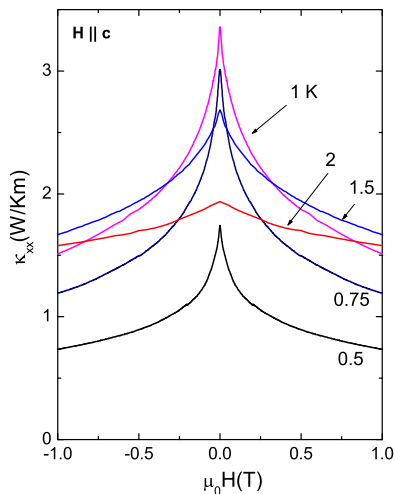


FIG. 7: Expanded view of $\kappa_{xx} \equiv \kappa$ vs. H in the vortex state of CeCoIn_5 ($T < T_c$). The sharp peaks in weak H arise from the field suppression of the broad peak in $\kappa(0, T)$ below T_c (see Fig. 1b).

finite field provided early key evidence that the peak in κ arises from enhancement of ℓ of nodal excitations in a d -wave superconductor. Similarly, the low-field peak reported here in κ_{xy} at 0.5 and 0.75 K (Fig. 3a) confirms that the cusp-anomaly in κ_{xx} is electronic in origin. The step increase in ℓ below T_c implies that the nodal qp does not experience the intense scattering from spin excitations. The close similarity between CeCoIn_5 and YBCO suggests that a steep enhancement of ℓ below T_c associated with nodal quasiparticles may be generic to electronic-mediated pairing with d -wave symmetry.

VIII. DISCUSSION

We have exploited the unusually large Righi-Leduc effect in CeCoIn_5 to determine the Wiedemann-Franz ratio

of its charge carriers at low T . As shown in Fig. 3, the 2 Hall conductivities κ_{xy} and σ_{xy} are strongly non-linear, with a change-in-sign of the curvature occurring as H increases from 0 to 12 T. Remarkably, over a broad interval of T , the 2 quantities may be scaled together using an H -independent Lorenz parameter $\mathcal{L}_H(T)$. We find that \mathcal{L}_H is weakly T dependent and close to the Sommerfeld value $(\pi^2/3)(k_B/e)^2$. The strict insensitivity of \mathcal{L}_H to field allows the electronic heat conductivity κ_e to be determined unambiguously. On subtracting κ_e from the observed κ_{xx} , we uncover a large background charge-neutral term κ_b that is field sensitive. As H increases, κ_b falls while σ rises in proportion. This implies that spin excitations are the dominant scatterers of the electrons.

The transport picture that emerges is that, throughout region I in zero H (Fig. 1a), the electrons are strongly scattered by spin excitations. Moreover, the spin excitations contribute the dominant share of the charge neutral thermal conductivity κ_b , which accounts for $\sim 45\%$ of the observed κ_{xx} at T_c . In a finite $\mathbf{H}||\mathbf{c}$, the density of spin excitations is strongly suppressed. This leads to 2 correlated effects. The neutral heat term κ_b is suppressed, while the 3 electronic currents σ , σ_{xy} and κ_e grow in proportion, as a result of strong enhancement of ℓ . The trend in κ_b suggests that the full suppression of spin scattering is attained when $H \rightarrow H_s$. An interesting scaling relationship between σ^2 and σ_{xy} is found. (Two recent findings related to this work are Refs. [22, 23].)

Acknowledgments

We thank Y. Matsuda, K. Behnia, and L. Taillefer for useful discussions. Y. O. acknowledges partial support by the Nishina Memorial Foundation. Research at Princeton University and the Brookhaven National Laboratory was supported by NSF (DMR 0213706) and by the U.S. Department of Energy (DE-Ac02-98CH10886), respectively.

-
- [1] Petrovic C. *et al.* J. Phys. Condensed Matter **13**, L337 (2001).
 - [2] Movshovich R. *et al.* Phys. Rev. Lett. **86**, 5152 (2001).
 - [3] Izawa K. *et al.* Phys. Rev. Lett. **87**, 057002 (2001).
 - [4] Ormeno R. J. *et al.* Phys. Rev. Lett. **88**, 047005 (2002).
 - [5] Aoki H. *et al.* J. Phys. Condensed Matter **16**, L13 (2004).
 - [6] Radovan H. A. *et al.* Nature **425**, 51 (2003); Bianchi A. *et al.* Phys. Rev. Lett. **91**, 187004 (2003); Kakuyanagi K. *et al.* Phys. Rev. Lett. **94**, 047602 (2005).
 - [7] Paglione J. *et al.* Phys. Rev. Lett. **91**, 246405 (2003).
 - [8] Bianchi A. *et al.* Phys. Rev. Lett. **91**, 257001 (2003).
 - [9] Bel R. *et al.* Phys. Rev. Lett. **92**, 217002 (2004).
 - [10] Onose Y., Li L., Petrovic C. and Ong N. P. Europhys. Lett. **79**, 17006 (2007).
 - [11] Kalychak, Y. M. *et al.* Russian Metallurgy **1**, 213 (2007).
 - [12] Krishana K., Harris J.M. and Ong N.P., Phys. Rev. Lett. **75**, 3529 (1995).
 - [13] Zhang Y. *et al.* Phys. Rev. Lett. **86**, 890 (2001).
 - [14] Durst A. C., Vishwanath, A. Lee P. A., Phys. Rev. Lett. **90**, 187002 (2003).
 - [15] Nakajima Y. *et al.* J. Phys. Soc. Jpn. **73**, 5 (2004).
 - [16] Zhang Y. *et al.* Phys. Rev. Lett. **84**, 2219 (2000).
 - [17] Paglione J. *et al.* Phys. Rev. Lett. **97**, 106606 (2006).
 - [18] Paglione J. *et al.* Phys. Rev. Lett. **94**, 216602 (2005).
 - [19] Tanatar M. A., Paglione J., Petrovic C., Taillefer L. Science **316**, 1320 (2007).
 - [20] Broholm C. *private communication*
 - [21] Sologubenko A.V. *et al.* Phys. Rev. Lett. **84**, 2714 (2000);

- Hess C. *et al.* Phys. Rev. Lett. **90**, 197002 (2003); Jin R. *et al.* Phys. Rev. Lett. **91**, 146601 (2003).
[22] Singh *et al.*, Phys. Rev. Lett. **98**, 057001 (2007).
[23] Izawa *et al.*, cond-mat/0704.1970.